Indentation Techniques in Nuclear Applications: A review paper

J. SPINO[2], W. GOLL[1] and E. H. TOSCANO[2]

[2] European Commission, Joint Research Centre, Institute for Transuranium Elements, PO Box 2340, 76125 Karlsruhe, Germany
[1] Framatome ANP GmbH, P.O. Box 3220, 91058 Erlangen Germany

Abstract

Indentation testing, in particular micro-indentation tests, is a straightforward method to determine several properties of irradiated materials. In fact, with this type of tests, material constants and fracture properties can be deduced from measurements performed on a relatively small surface, which constitutes an important advantage when dealing with highly radioactive specimens. On the other hand, since the material response to indentation is complex, with the occurring elastic and plastic deformations being affected by radiation damage, impurities and temperature variations, careful analysis of the data is required.

In the nuclear field, materials of direct interest range from carbide-, nitride- and oxide-fuels, to diverse ceramic and glasses utilised for the immobilisation of high level nuclear waste, as well as simulated fuels and fuel-rod cladding materials, the later which are tested to analyse the loss of ductility after irradiation and its recovery after high temperature annealing.

This paper describes the most common indentation techniques and the essential properties that can be determined by these techniques. A review of the main results obtained by indentation testing in fuels, waste glasses and cladding materials is also provided.

1 Introduction

Indentation testing, in particular micro-indentation methods, is a simple technique to test several properties of irradiated materials. From this type of tests, the evolution of mechanical constants and fracture properties of the material can be deduced from relatively small measuring areas, which constitutes an important advantage when dealing with highly radioactive specimens. However, since the response of the material to indentation is complex, involving elastic and plastic deformations that are affected by radiation damage, impurities and temperature changes, careful analysis of the results is needed.

In the nuclear field, the range of materials of direct interest for the application of the technique is wide, running from carbide-, nitride- and oxide-fuels, to diverse ceramic and glasses utilised for the immobilisation of high level nuclear waste, as well as to simulated fuels from which the influence of fission products is obtained, and cladding and guide tube materials whose ductility loss during irradiation must be monitored.

In the following sections the main techniques that have been successfully applied to determination of several constants and properties of nuclear materials are described. Highlights of the results obtained in each case are also given.

2 Indentation techniques

2.1 Hertzian indentation

In the Hertzian indentation a spherical indenter is pressed at a given loading rate onto the polished surface of a specimen, until a ring crack is formed at a critical load, P_c (Fig.1) In practice, the evaluation from these tests of the fracture toughness, K_{Ic}, depends on a number of quantities, in addition to the critical load for crack formation, P_c, and the ring crack radius, r [1, 2].

[1] Phone +49 913 11 89 49 74, Wolfgang.goll@framatome-anp.com
[2] Phone +49 72 47 95 14 09, toscano@itu.fzk.de

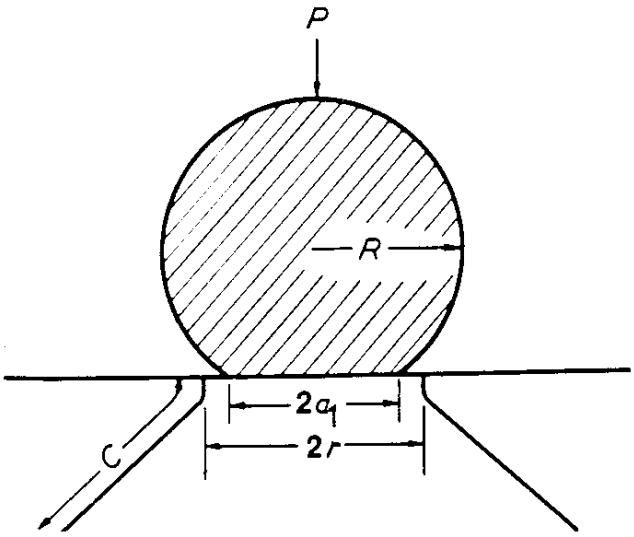

Fig. 1 Hertzian indentation and affected zone dimensions [1]

When such a spherical indenter is pressed onto the surface of a brittle elastic material, a complex stress field is set up under and around the indenter. This stress field was first described by Hertz [3]. Auerbach [4] showed later that ring cracks with radius r form around the area of contact between indenter and specimen (contact radius $a_1 < r$) (see Fig. 1). From Auerbach's treatment it results that the critical load P_c for ring crack formation is proportional to the indenter radius, R, i.e.

$P_c = AR$

such that the proportionality constant A is linearly dependent on fracture surface energy, γ, of the material to be analysed. This is the so-called Auerbach's law. Since it is fulfilled that

$K_{IC} = (2 \gamma E/(1-\nu^2))^{1/2}$

where E and ν are respectively the Young's and Poisson's moduli, for ideally brittle materials, hence, in the absence of any permanent plastic deformation, the fracture toughness, K_{IC}, can thus be obtained from P_c measurements. This implies, however, knowledge of the correlation 'A vs. γ', which depends on several material- and crack-extension constants [1]. On increasing the load, the ring cracks extend in a cone-shaped form into the specimen (Fig. 1). The cracks are therefore often also referred to as cone cracks.

2.2 Vickers indentation

In the Vickers indentation a sharp square-pyramidal indenter with an apex-angle of 136 ° is pressed into the sample at a given load, P, with a typical dwell-time of 10 seconds. The material of the indenter is typically diamond. For high temperature tests, sapphire indenters are currently used. A scheme of the test, with the characteristic cross-section and surface views and the corresponding deformation fields and crack pattern, as described in Ref. [5], is shown in Fig. 2. Apart from the applied load, P, the main characteristics dimensions of these tests are the half-diagonal length of the impression left after load removal, a, and, in brittle materials, the length of the (post-indentation) cracks formed at the print corners, c, as measured from the centre of the indentation print (Fig. 2). The characteristic quantities obtained from these tests are the material hardness, H, and, in crack-prone materials, the fracture toughness, K_{IC}. The first of these parameters is obtained solely from the measurement of the print half-diagonal length. The second one is obtained from both the print half-diagonal and the average crack lengths. The corresponding expressions for the parameters H and K_{IC} are respectively:

$H\ (Kg/mm^2) = 1.8544\ P/(2a)^2$ and $K_{IC}\ (MPa.m^{1/2}) = 0.057\ H\ a^{1/2}\ (E/H)^{0.4}\ (c/a)^{-3/2}$,

where E is the Young's modulus of the tested material

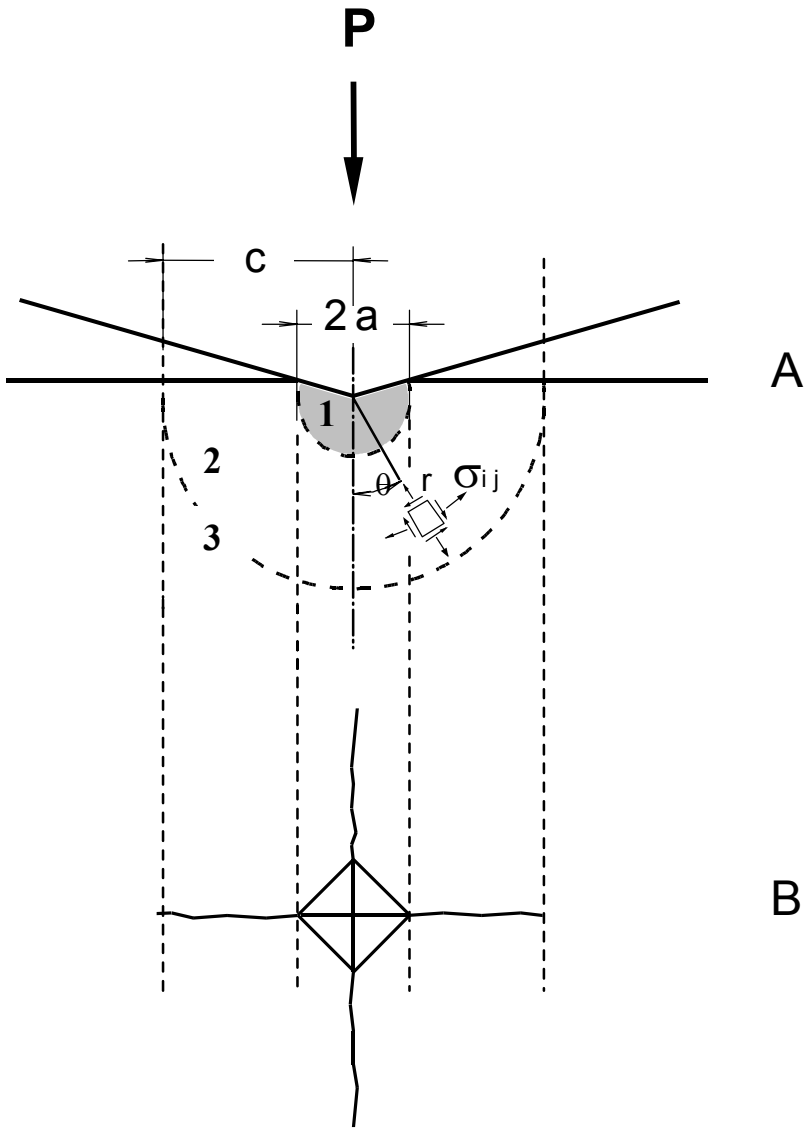

Fig. 2 Vickers indentation cross-section **(A)** and surface view **(B)**, with corresponding deformation fields and crack pattern

P = applied load, a = imprint half-diagonal length, b= crack length accounted from the imprint centre), (r,θ) = polar co-ordinates, σ_{ij} = polar stress-field components. 1= plastic domain, 2 = elastic domain (also containing the fracture process), 3 = median or half-penny crack boundary underneath the indentation.

It is to be remarked that the Vickers test has become a standard technique for materials characterization not only for research, but also for production purposes. Definite advantages of it are its simplicity and the small amount of sample required. Thus, available correlations for metallic materials between, e.g., the hardness and the yield stress (σ_y), and existent validations of the Vickers-K_{IC} values for brittle materials compared to those of more expensive and complicated tests (as e.g., the two or three-point bend tests), make the technique very attractive even for routine process- and property checks, for a wide variety of materials.

2.3 Knoop indentation

In the former sections it was shown that a key parameter for the determination of the indentation fracture toughness, K_{IC}, is the Young modulus of the material, E (see section Hertzian indentation); which in the case of the Vicker's indentation reduces to the ratio E/H, where H is the hardness of the material (section 2.2). The E/H ratio can be determined from the Knoop indentation, which utilizes a strongly asymmetric rectangular-pyramid indenter, where the long diagonal, a, is 7.11 times larger than the short diagonal, b. A scheme of the Knoop indentation print is shown in the top-right portion of Fig. 3. The method is based on a suggestion of Marshall et al [6] that under this geometry the extent of the elastic recovery of the print diagonals after indentation is a linear function of the H/E ratio. Indeed, whereas the relaxation of the print diagonals in a Vicker's indentations is isotropic; in a Knoop indentation only the shorter diagonal shows elastic recovery, while the longer diagonal remains relatively unaffected. Since for rigid/plastic materials (low H/E) the recovery is almost zero and for highly elastic materials (high H/E) it is the largest, Marshal et al [6] proposed that the residual diagonal ratio might be expressed as:

$b'/a' \cong b'/a = b/a - \alpha\,(H/E)$

where α is a calibration constant.

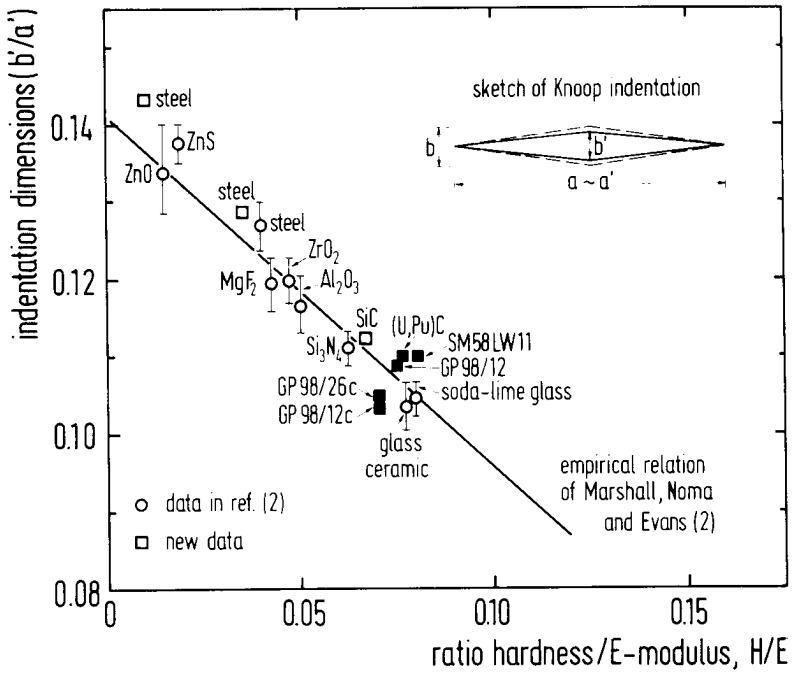

Fig. 3 Calibration curve b'/a' vs. H/E after Knoop indentation in different kinds of materials, from Ref. [1] p. 1105

The above calibration curve as obtained by Marshall et al. [6] (circles) is shown in Fig. 3 according to description given in Ref. [1] (p. 1105). The figure includes also latter data on waste glasses and carbide fuel materials, as described in Ref. [1] (p. 1105) (squares). In both cases, good fitting of the results was obtained for α= 0.45. Since H is measured by indentation as well, the value of E can be easily obtained from the constant α, using for instance Hertzian or Vickers indentation. Marshall et al. [6] quoted for this procedure an accuracy better than 10%, using α= 0.45.

3 Material Properties

In the previous sections we have pointed out that beside the elastic modulus, E, the main material parameters that can be determined by indentation are the hardness, H, the fracture toughness K_{IC}. In this

section, we briefly describe the meaning of these quantities and their possible correlation to other material properties.

3.1 Hardness

Hardness is one of the most important parameters for engineering materials evaluation. Ever since the 19th century, relative hardness values have been derived on the aptitude of minerals to scratch other minerals. In this sense, the Mohs-scale, devised by the German mineralogist G. Mohs in 1812, was the first attempt to classify materials in a systematic way, by observing whether the surface of given substance was scratched by a substance of known or defined hardness.

In the more modern study by D. Tabor [7], the hardness is defined as the aptitude of a material to resist plastic deformation. According to this author, even for brittle materials, which after indentation develop characteristic cracks beyond the affected plastic zone (Fig. 2), the permanent deformation left after load removal is a measure of their plasticity. This is because it is believed that even for hardly deformable materials certain movement of dislocations is activated under the high stresses of the indentation test, which otherwise remains forbidden under the conditions of usual compressive tests. Thus, the hardness number can be utilized as a reference of the hindering of the dislocation movement, e.g., after mechanical work, alloying, secondary phase precipitation, or irradiation processes; or in the opposite way as a reference of their improvement, e.g., after annealing processes.
In addition, as mentioned in section 2.2, for metallic materials, various correlations exist between the hardness and the corresponding yield (σ_y) and rupture (σ_r) stresses. Also as described in section 2.3, for both metallic and ceramic materials a correlation between the hardness and the E-modulus is possible. Finally, for ceramic materials the hardness can be correlated with the strength reached after the sintering process, which is also a measure of the quality of the material.

Fracture toughness (K_{Ic})
This parameter describes the resistance of a material against *fracture propagation* or, in other words, against the creation of new surfaces by fracture. It is appropriate for the characterization of ceramic and glass materials, and also applicable to metals, for instance for the characterization of stress-corrosion-cracking (SCC) processes.

Starting from the quantity K_I, which is the stress intensity factor or stress increase at the tip of a single crack formed in an homogeneous material, the critical stress intensity factor, or fracture toughness, K_{Ic}, is thus defined as the K_I-level at which critical crack extension occurs, such that:

$$K_I \geq K_{Ic}$$

Both quantities have a dimension that is hardly intuitive and of difficult interpretation, namely: force/(length)$^{-3/2}$, i.e., MNm$^{-3/2}$ or MPam$^{1/2}$.

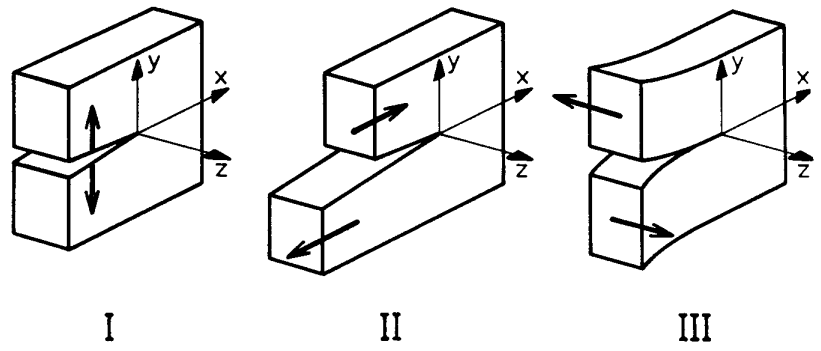

Fig. 4 Fundamental types of crack-openings occurring in a material [1]

The designation I in K_{Ic} indicates the relevant type of crack opening applying in this case. As seen in Fig. 4, which shows the main possible types of crack-openings in a material, the type I crack opening is that

occurring under tensile conditions, along the plane perpendicular to the applied stress. This is the case of highest technological importance [1]. Whereas K_I is strongly dependent on specimen dimensions, K_{Ic} is (ideally) a material constant independent of specimen geometry and is, therefore, a measure of the resistance of the material against fracture.

Since 1970, various norms have been issued to measure K_{Ic}, e.g., ASTM-E-338-81, E-399-83, E 602-81, based on the use of different types of pre-notched specimens (i.e., compact specimens, arc-shaped specimens and disc-shaped specimens), for which the analytical expression of the stress intensity factor (K_I) is known. However, for highly active specimens, most of the above methods are not suitable, because large specimens and several tests are required. In addition, since as mentioned in section 2.2 validation tests exist demonstrating the excellent agreement between the indentation-K_{IC} values and those from standard tests, the indentation K_{IC} measurements appear as mostly appropriated for nuclear materials characterization. This last particularly in view that only small sample surfaces are required (< 1 cm²), at the time that tenths of tests can be easily performed in reasonable short time.

4 Results

In this section, the results of specific applications of the indentation techniques to some nuclear materials are described.

4.1 Fuels

4.1.1 Microhardness and fracture toughness of irradiated LWR-fuels by Vickers indentation

The micro-hardness and fracture toughness of different LWR-UO_2-fuels with average burn-ups in the range 40-100 GWd/tU were systematically investigated at ITU, via numerous Vickers indentations performed at close intervals (~ 50 µm) along different radii of the fuels, exploring influences of the indentation load, burn-up and porosity [5].

An example of these results in terms of K_{IC} is shown in Fig. 5, which illustrates the radial evolution of the fracture toughness of a LWR-fuel with an average burn-up of roughly 40 GWd/tM. The fuel in question showed a narrow but well developed high-burn-up (rim) zone at the periphery, of about 100 µm in width. As seen in the figure, two characteristic regions can be distinguished in the fuels, namely a predominant central (and intermediate) zone with a K_{IC}-value nearing that of non-irradiated UO_2, and the rim region in which this value increases by almost a factor 3.

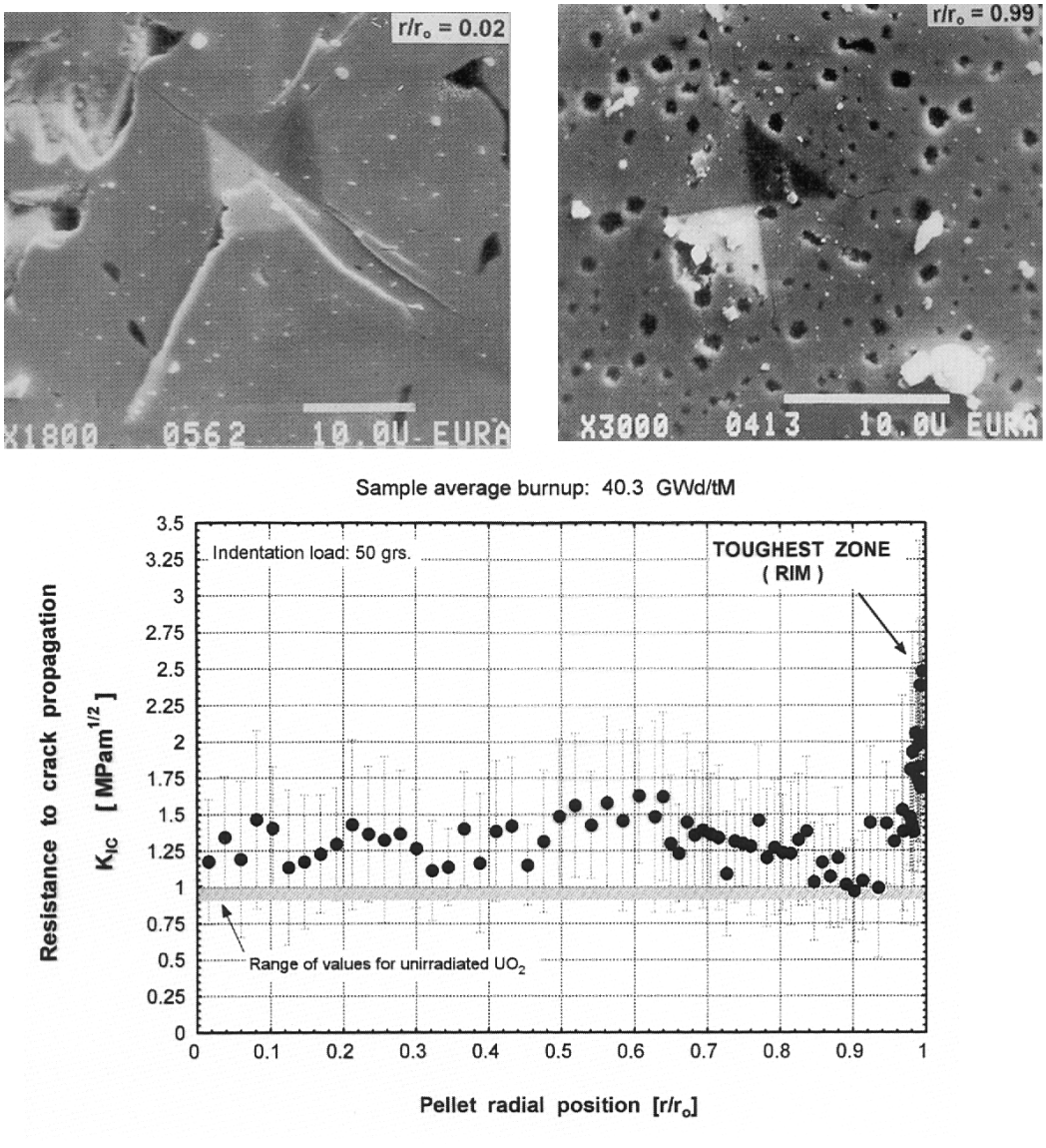

Fig. 5 Fracture toughness of a LWR-fuel with 40.3 GWd/tM burn-up as a function of the pellet radius as determined by Vickers indentation (bottom). Typical indentation prints micrographs in the fuel centre and in the fuel periphery (top left and right)

As can be seen also in the micrographs of Fig. 5, the above behaviour is manifested by an increase of the indentation diagonal length (softening sign), plus a considerable shortening of apex-crack lengths in the rim zone (toughening sign), both leading to a definite increase of the K_{IC} in the region, probably due to the formation of micro-cavities in the fuel. These observations have been repeated in all other fuels examined. This has lead to the conclusion that the formation of the high burn-up rim-structure would bring about improvement of the mechanical behaviour of the fuel, namely in that the softer and tougher zone formed at the fuel periphery would act as a buffer absorbing the mechanical stresses caused under power-ramp or PCMI conditions. (PCMI=Pellet Cladding Mechanical Interaction).

4.1.2 Elastic constant of doped UO_2 by Knoop indentation

As an example of application of the Knoop indentation method to nuclear fuels, we briefly describe in this section the recent results obtained in this way of the elastic constants of UO_2 fuels with simulated burn-ups of up to 200 GWd/tM [8]. Fig.6 shows thus as a function of burn-up the E-modulus values obtained via indentation, i.e. by combination of the H-values obtained by the Vickers method with the H/E-values obtained by Knoop method (sections 2.2. and 2.3) (closed symbols), in comparison with the E-values obtained by measuring the compressibility of these materials by synchrotron diffraction under high-

pressure (open symbols). A reasonable agreement between both types of results is therefore visible (Fig. 6), indicating that the elastic constants of UO_2 are systematically increased in the course of irradiation as fission products replace the fissioned U-atoms in the lattice. According to the Grüneisen relation, the observed increase of the stiffness of the fuel-lattice with burn-up is also consistent with the corresponding decrease of the thermal expansion measured by high temperature X-ray diffraction [8].

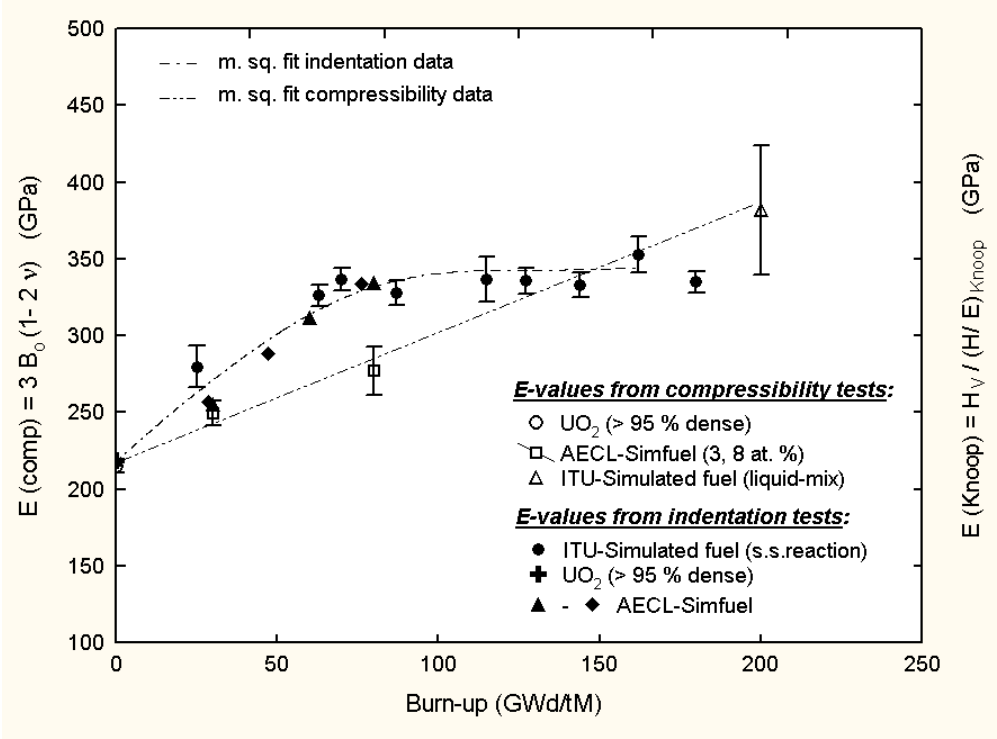

Fig. 6 Comparison of E-modulus values obtained by compressibility and indentation tests [8]

4.2 Waste immobilisation

For the safe long-term storage of the liquid radioactive wastes originating from the reprocessing of nuclear fuels, their immobilisation in a glass matrix and subsequent storage in underground repositories is the most accepted concept worldwide [9]. In this context, one of the important questions refers to the stability of the glass matrix under the sustained radiation damage (particularly from γ-decays) arising from the enclosed fission products and actinides, whose effect extends over thousand of years. For the simulation of this global damage in a shorter time-scale, curium containing glasses have been produced to simulate different damage levels in the history of the glass, and have been tested by Vickers indentation to monitor the evolution of the K_{IC}-value with the dose; this last parameter being taken as indicator of the mechanical stability of the glass-matrix [9].

Fig. 7 thus shows the correlation between the simulated and the real time scales in terms of the accumulated α-damage (α-decays/m³) for the two different Cu-concentrations used. The results of the Vickers indentation tests performed are summarized in Fig. 8, showing the measured crack-lengths and the corresponding probability to failure (by cracking) as a function of the cumulative γ-dose. The results showed no deterioration but an improvement of the toughness of the glasses with the γ-dose, leading to an increase of the K_{IC}-values of up to 100 % at the highest doses [9]. Among the different physical and microstructural changes produced by radiation damage, the observed toughening effect by the α-dose, also previously observed in other nuclear waste glasses and ceramic matrixes [10], might be due to the formation of He-bubbles by the ionizing radiation [9]. In this aspect, the effect would be similar to that described in section 4.1.1 with regard to the increase of the K_{IC}-values in the rim zone of high burn-up fuels, where also a possible reason is attributed to the formation of micro-cavities in the region [5].

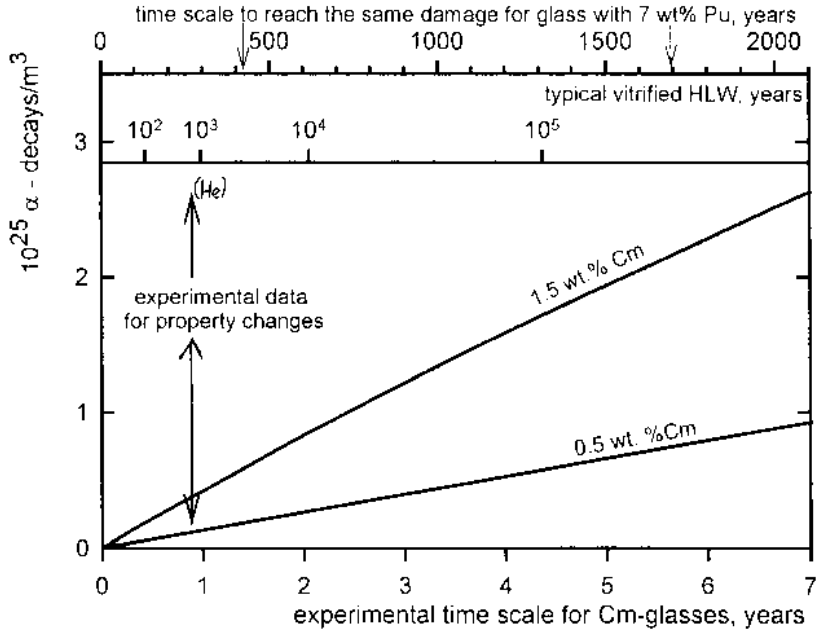

Fig. 7 Relation between accumulated α-damage and the storage time for two different Cm-concentrations in curium-doped waste glasses [9]

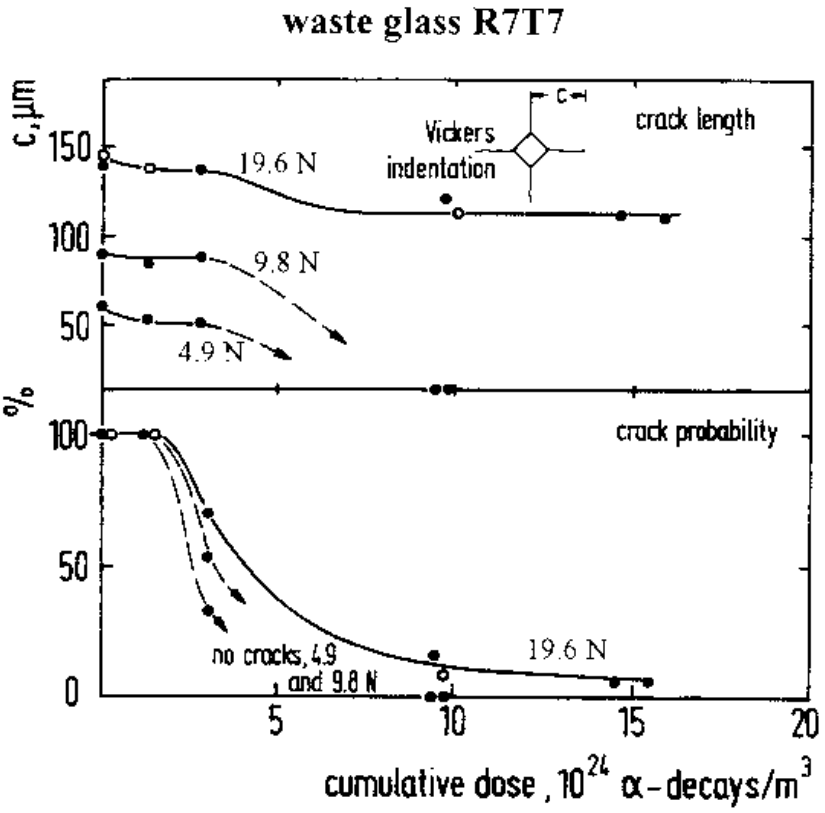

Fig. 8 Vickers-indentation cracks and probability to failure as a function the cumulative a-dose in curium-doped waste glasses [9]

4.3 Cladding materials

To follow the evolution of the mechanical properties of LWR-fuel cladding materials with burn-up, Vickers hardness tests have been started to monitor the ductility loss of this material under irradiation and its recovery by thermal annealing under different conditions. Preliminary results of these tests are shown in Fig. 9, illustrating a series of indentations across the cladding wall of a high burn-up fuel. The figure shows that two zones are clearly differentiated by the test, namely the main cladding exhibiting considerable hardening with respect to the starting material, and the softer inner liner that was introduced for improving the PCI-performance. Although not completely visible at the magnification of Fig. 9b, a closer look at the imprints in the irradiated cladding permits differentiating certain hardening gradients across the wall. This behaviour may reflect a variation of the fine metallurgical parameters of the material.

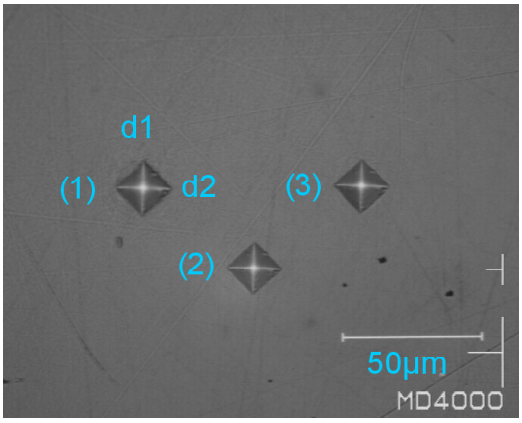

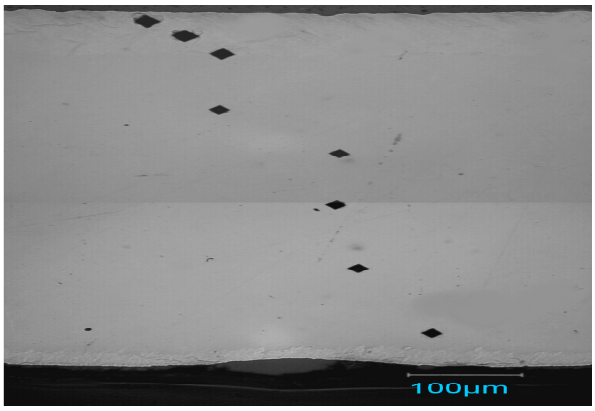

water side fuel side

Fig. 9a Standard calibration sample (starting cladding material)

Fig. 9b Irradiated cladding with inner liner

Fig. 9 Vickers indentation tests in a LWR-fuel cladding material with inner liner, before and after irradiation

5 Conclusions

Different applications of Vickers, Knoop, and Hertzian indentation tests have been presented, as well as the main mechanical parameters obtained from them have been explained. Particularly for nuclear applications, because of its simplicity and the small amount of material required, it emerges that indentation tests are very useful not only for routine checks but also for prediction purposes. As for the predicted properties, the demonstrated improvement of the indentation toughness of fuels and waste glasses with respectively increasing burn-ups and γ-dose exposures appeared thus of especial technological importance.

With respect to the type of tests, it is concluded that the Vickers indentations are mostly recommendable for hardness and fracture toughness characterizations, while the Knoop indentations are indispensable for elastic-properties determinations.

References:

[1] Indentation Fracture and Mechanical Properties of Ceramic Fuels and of Waste Ceramics and Glasses. Hj. Matzke Ed., European Applied Research Reports: Nuclear Science and Technology, 1987, ISBN 3-7186-0443-4

[2] Indentation techniques, Hj. Matzke and E. H. Toscano Eds., European Applied

Research Reports: Nuclear Science and Technology, Vol. 7 (1990), 0379-4229/89/1335-1504

[3] H. Hertz, On the contact of elastic solids, Zeit. Reine u. Angew. Mathematik, 92 (1896) 156. Translation in Hertz's Miscellaneous Papers, Mac Millan, London, UK, 1896, pp146-162

[4] F. Auerbach, Ann. Phys. Chem., 43 (1891) 61

[5] J. Spino, J. Cobos-Sabate and F. Rousseau, J.Nucl.Mater. 322 (2003) 204

[6] D. B. Marshall, T. Noma and A. G. Evans, J. Am. Cer. Soc. 65 (1982) C 175

[7] D. Tabor, Br. J. Appl. Phys. 7 (1956) 159-166

[8] M.C.Pujol, M.Idiri, L.Havela, S.Heathman and J.Spino, J. Nucl. Mater. (2004) 189

[9] Hj. Matzke and E. H. Toscano, in Ref. [2] p 1403.

[10] W. J. Weber and Hj. Matzke, in Ref. [1] p 1221